17th World Conference on Earthquake Engineering, 17WCEE
Sendai, Japan - September 13th to 18th 2020

RESILIENT DESIGN OF RC-BUILDINGS WITH HYSTERETIC ENERGY DISSIPATION DEVICES IN SOFT SOILS

H.J. Nangullasmú-Hernández [(1)], A. Tena-Colunga [(2)]

[(1)] *PhD, Posgrado de Ingeniería Estructural, Universidad Autónoma Metropolitana Azcapotzalco, Ciudad de México, e-mail: hnangu@hotmail.com*
[(2)] *Professor, Departamento de Materiales, Universidad Autónoma Metropolitana Azcapotzalco, Ciudad de México, e-mail: atc@correo.azc.uam.mx*

Abstract

In this paper, the authors propose a resilient design methodology for reinforced concrete buildings with intermediate moment-resisting frames (RCB-IMRFs) and hysteretic energy dissipation devices (HEDDs) mounted in chevron steel bracing. The design methodology is focused on stiffness ratios between the different structural systems (frames, bracings and HEDDs). The buildings ranged from 8 to 24 stories using the suitable stiffness ratios "α" according to their global slenderness ratios. In order to test the designed buildings in a demanding scenario close resonant responses, the models were located where a greater probability exist that the period of the structure would be shorter but close to the soil's natural period (T_s). Due to the soil properties of the lakebed zone of Mexico City, soil-structure interaction (SSI) was modeled using as a set of point springs according to NTCS-04. Furthermore, different HEDDs for each analysis direction were used (ADAS and BRBs), in order to compare their structural performance based on structural geometry configuration, stiffness ratio between the HEDD and the bracing system (β) and local ductility developed (μ_d). In addition, extra confinement requirements were included to the typical detailing established in Mexican codes for RC-IMRFs, favoring satisfactory design mechanisms when the HEDDs develop most of their nonlinearity (structural fuse). In first instance, pushover analysis were performed in order to obtain global capacity curves and inelastic demand mappings with two different lateral load patterns, based upon a static load distribution and the fundamental mode of vibration. These results were useful to validate the global seismic parameters used in the design process. In second instance, inelastic dynamic analysis were performed for complete 3D designs according to the code, in order to obtain hysteretic cycles developed by the global structure, story drifts related to different limit states, inelastic demand mappings, envelopes of peak and average response. The results were obtained from eight pairs of acceleration records, representative of the site where the buildings are located, and simultaneously applied in order to assess the maximum inelastic response. Finally, commentaries are made regarding to inelastic hysteretic cycles, residual drifts, residual drift ratios, mappings of residual deformations in HEDDs and residual rotations in RC elements. From the results obtained, it is noticeable that when a suitable stiffness ratio among the different structural systems are considered and a story drift is set, a resilient structural performance is feasible for RCB-IMRFs with HEDDs.

Keywords: Energy dissipation, metallic fuses, seismic response control, resilient design

1. Introduction

With the population increase in large cities, a resilient design methodology is necessary to warrant not only the safety of its occupants, but also minimizes damage to their buildings. Construction codes in Mexico focus on preserving people lives based on the seismic dissipation energy through the controlled damage of its main structural elements, associated with stiffness and strength degradation for those elements. The structure could take certain amount of damage depending on the building importance, but this structural design philosophy could result in activities suspension for months or even years while the repair project is being carry out, for cases where this is feasible.

In Mexico City, after the September 19, 1985 earthquake, the seismic response control was an attractive solution for engineers of that time and it was used to retrofit few buildings located in soft soils [1]. During the September 19, 2017 earthquake in Mexico, a resilient structural behavior was observed in these buildings because the damage was focus on the "metallic fuses", while the others structural elements did not take visible damage and minimal reparations works were implemented (Fig. 1).

Fig. 1 – Izazaga 38-40 building

Mexican building codes did not mentioned energy dissipation devices before 1995. After this year, if some structural engineers wanted to implement energy dissipation devices, they were demanded to demonstrate their efficiency to the competent city authority [2]. Until 2017, some seismic design parameters, associated with deformation capacity of the structure and drifts limits for service and ultimate condition, were proposed for the Mexico City Building Code. However, in this code global design parameters for the seismic design using a traditional code-oriented procedure are not provided for any energy dissipation device system, except for Buckling Restrained Braces (BRBs) [3], with no reference of the studies in which these global design parameters are justified.

With the purpose to promote the construction of reinforced concrete buildings with intermediate moment-resisting frames (RCB-IMRFs) and HEDDs (Hysteretic Energy Dissipation Devices), which are not exclusive for BRBs, the authors have developed in the last 10 years a resilient design methodology based on a large parametric study, which it takes advantage of previous results [4, 5] and recommendations done by practicing engineers [6, 7] in order to choose different structural and geometric parameters, such as minimum ductile-confinement requirements for RC elements and different HEDDs, height of the buildings, angles of inclination of the braces with respect to the horizontal plane, among other parameters, as explained in following sections.

2. Description of the buildings under study

The buildings under study are for office use with four bays of 800 cm at *x*-direction and three bays of 700 cm at *y*-direction (Fig. 2a). The floor system is composed of a reinforced concrete slab 10 cm thick and secondary beams (30x45 cm) disposed in both directions for a better vertical load distribution. The height for all the stories is 400 cm, which caused different angles for the steel braces in each analysis direction ($\theta_x \approx 45°$ and $\theta_y \approx 49°$). The different colors in Fig. 2 denote different mechanical or geometrical properties for the structural elements. Furthermore, the cross sections changed as the building increases in height (Fig. 2b and 2c), a common design strategy used in Mexican design firms to optimize sections and reduce the total weight of the structure. Nevertheless, there are not changes of cross-sections for beams, columns, and bracings in the same story, in order to prevent the formation of clear weak or soft stories.

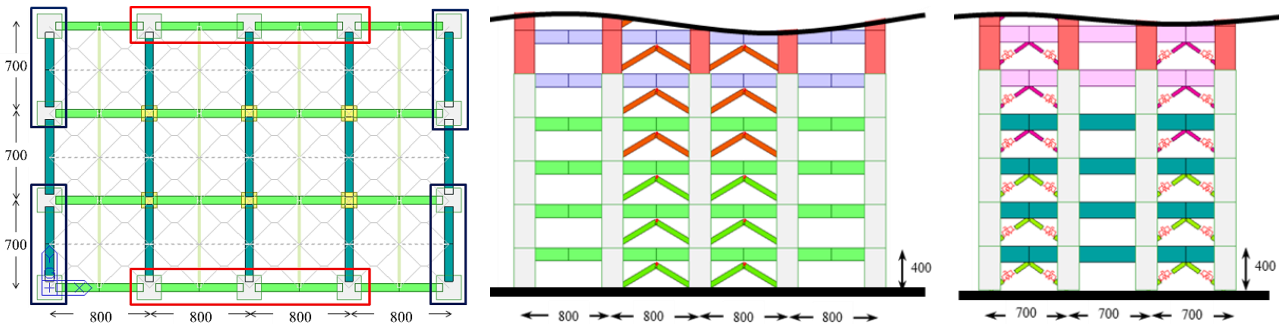

a) Plan view b) X-direction c) Y-direction

Fig. 2 – Geometrical configuration for all the models evaluated (units: cm)

The models have eight, 15 and 24 stories, in order to evaluate different slenderness ratios. The 15 and 24 story models do not satisfy the global slenderness regularity condition (H/L<2.5). Consequently, the design spectrum underwent a reduction in $Q´$ (the equivalent of the R_μ factor of US codes) by multiply it by the irregularity correction factor of 0.9. The initial elastic stiffness ratios used for all the buildings are shown in Table 1. From this table, it is appreciated that the value of "α" is always greater in the *y*-direction because its slenderness ratio. In addition, as the height of the models increases, the "α" parameter used increases as well. With these proposed balances, it was found in previous studies that yielding of beams and columns could avoided or minimized when HEDDs develop their maximum target design ductility [4, 5]. Finally, stiffness ratios between the HEDDs and braces (β) were different for each analysis direction, in order to evaluate the behavior of two different HEDDs. For the bays marked with a red rectangle at the *x*-direction (Fig. 2a), ADAS devices were used, as they are representative of β = 0.50. For the bays enclosed in a blue box, BRBs were used, which are representative of β= 1.0.

Table 1 – Stiffness ratios for the buildings under study

	α_x	α_y	β_x	β_y
8-S	0.25	0.35	0.50	1.00
15-S	0.35	0.50	0.50	1.00
24-S	0.50	0.65	0.50	1.00

2. Design of RC buildings with HEDDs

The general design procedure for RC buildings with HEDDs is schematically resumed in Fig. 3. The selection of a design seismic coefficient from the response spectrum is the first step, as well as the estimation of the fundamental period of the structure with the following formula obtained from previous parametric studies [8]:

$$T_{est} = (H/L)^{0.35} \quad (1)$$

where, H/L is the slenderness ratio for the entire building. The proposed seismic response modification factors for ductility (Q) and overstrength (R, equivalent to Ω_0 in US codes) reduce the elastic design spectrum. Then, the structural engineer must select the parameter α, which is the stiffness ratio between the frame and the bracing-HEDD system. The "optimal" selection of this parameter depends on the slenderness ratio of the building. As the slenderness ratio increases, the frame system must provide a greater initial elastic stiffness in order to obtain a resilient structural design [4, 5].

As a first design iteration, only RC frame elements are taking into account for the analytical model of the building, in other words, the parameter α reduced the basal shear computed in the previous step, because the bracings and HEDDs do not provide lateral stiffness in this step. Strength and service requirements, specified by the Mexican codes for RC-IMRFs with the use of load combinations, checked the preliminary design for beams and columns [9]. Moreover, minimum ductile confinement requirements were taking into account to

the design process in order to increase the rotation capacity for RC elements. These requirements are associated with the increase of rebar diameter of the stirrups, as well as the decrease in the separation between them [9]. Likewise, the structural engineer must use a capacity design to warrant a strong column - weak beam mechanism for the frame. Besides, it is important to mention that the consideration of accidental eccentricity of 5% with orthogonal effects (100:30) rule is important to consider.

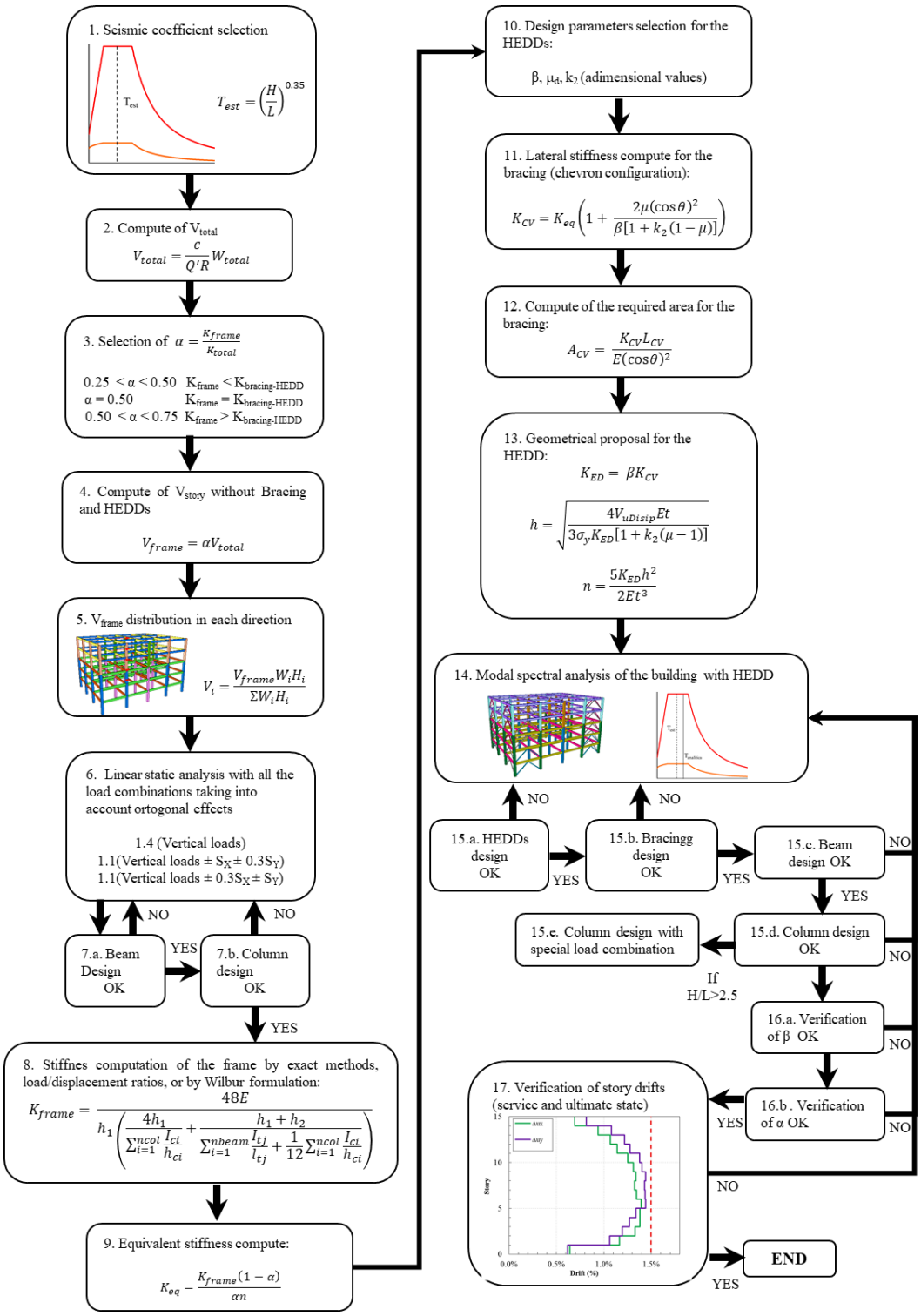

Fig. 3 – General design procedure for RC buildings with HEDDs

Once the pre-design of beams and columns is completed, the frame lateral stiffness should be assessed using approximate or exact methods, in order to assess the initial elastic stiffness for the bracings and HEDDs and pre-design them (steps 9 to 13, Fig. 3). An initial stiffness ratio β is useful to design specific HEDDs geometries. The first iteration for the HEDD's height is function of its elastic lateral stiffness and its peak local ductility, as well as the mechanical properties of the fabricated material. Finally, the number of plates (ADAS, TADAS), web area (shear panel) or the required axial area (BRB), depend on the device of interest proposed. With all the structural elements predesigned, a complete 3D analytical model (beams, columns, bracings and HEDDs) is used to perform modal spectral analysis according to the code, in order to start the final iterative procedure to achieve the final design. In this work, ADAS devices were modeled considering all the components of the stiffness matrix [10]. Furthermore, the design for BRBs was done according to what was proposed by Vargas and Bruneau [11]. To warrant a resilient structural design, HEDDs must be the structural seismic fuses of the entire system. Nevertheless, beams should act as a second inelastic defense if necessary (for example, earthquake motions that may surpass substantially the elastic design spectrum). The bracing and the columns must remain elastic within all the seismic excitation, so then, a special load combination in for corner and perimeter columns was proposed only for slender buildings (H/L>2.5).

Due to the soil properties of the lakebed zone of Mexico City, soil-structure interaction (SSI) is extremely important to consider. Buildings under study had different numbers of underground floors, according to current design practices in Mexico City. For example, the models of 8, 15 and 24 stories respectively had two, three and five parking levels below the ground level (Fig. 4a, 4b and 4c). Each parking level has a height of 400 cm. Perimeter RC walls border all the parking stories and the use of point-bearing piles constitute the foundation below the mat slab for each building. The length of the piles for the 15-story and 24-story are until the hard rock layer, which differs according to the zone where each building is located. A set of point springs in the foundation zone depict the SSI (Fig. 4), and the stiffness, as well as damping coefficients, were computed according to Appendix A of the seismic provisions for Mexico City [12].

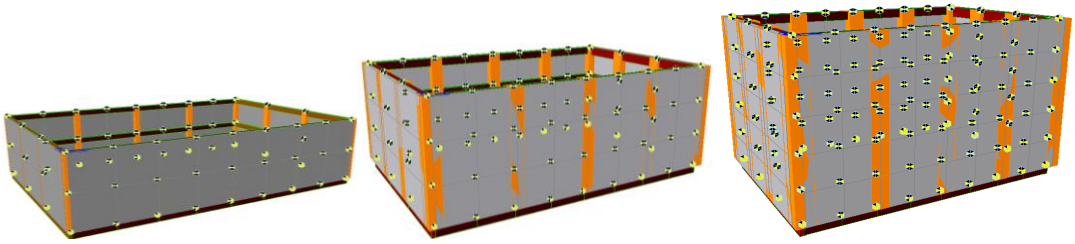

a) 8-Story b) 15-Story c) 24-Story

Fig. 4 – Soil-structure interaction for all the models under study

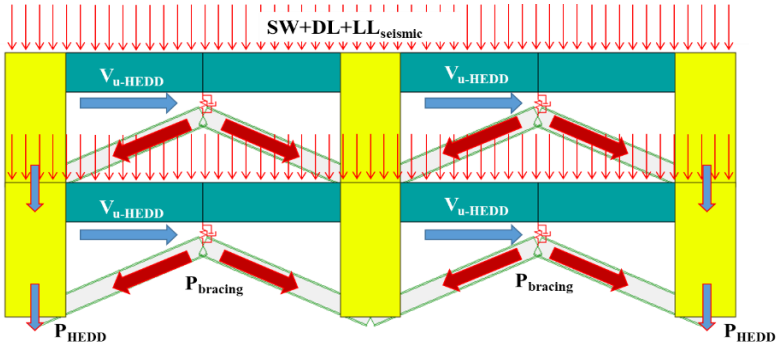

Fig. 5 – Special load combination for columns in slender buildings with HEDDs

From inelastic demands mappings of RC frames; exterior columns developed incipient yielding in slender buildings when the HEDD developed its peak local ductility [4, 5]. RC frames with steel bracing but without HEDDs have a similar undesirable effect [13], thus, in order to prevent such undesirable yielding, a special load combination was proposed and assessed for the design of exterior columns in slender buildings

(H/L>2.5). This new load combination takes into account the contribution of the gravitational load generated by self-weight, dead load and the live load used for seismic design (Fig. 5). In addition, the design shear of the HEDDs are considered ($V_{u\text{-}HEDD}$), which will be projected first to the bracings as axial load ($P_{bracing}$) and then to the column (P_{HEDD}). Once the strength requirements of all the elements are checked, the stiffness ratios β and α must be within a similar range to those proposed in the initial steps (Table 2). Otherwise, the structural engineer must repeat the conditions of the analytical model since the step 14 (Fig. 3). Moreover, the story drifts related to service (Δ_y) and ultimate state (Δ_u) should be checked also. If all the requirements fulfill, the design process of the building is completed.

Table 2 – Geometrical properties for HEDDs in 15-story model

HEDD	ADAS (X-direction)				BRB (Y-direction)					
	h (cm)	t (in)	Plates	β	L (cm)	t (in)	h (in)	Cross Section	Area (cm²)	β
D1 1-3	30	2	10	0.48	125	1.250	6.000	+	86.69	0.98
D2 4-7	25	2	9	0.52	120	1.125	5.500	+	71.67	0.97
D3 8-11	25	1.75	8	0.50	105	1.000	4.125	+	46.77	0.99
D4 12-13	25	1.625	5	0.50	85	0.750	4.500	-	21.77	0.99
D5 14-15	15	1.25	4	0.51	80	0.625	2.750	-	11.09	0.99

3. Final design for RC elements

For all building models, A-36 steel was used for chevron bracing. RC beams and columns were designed assuming a compressive strength for the concrete f'_c = 24.50 MPa (250 kg/cm² or 3550 psi) for eight and 15 story models. For the slenderest model, this value was increased to f'_c = 29.40 MPa (300 kg/cm² or 4270 psi), in order to satisfy the minimum requirements of heights and clearings.

Table 3 – Rebar arrangement for RC elements in the 15-story building (units: cm)

	Story	B	h	Rebar at top	Rebar at bottom	End stirrups	Center stirrups
Beams	V1x 1-4	50	100	7 No.10 + 2 No.8	7 No.10 + 2 No.8	4 No. 3 @ 10	4 No. 3 @ 20
	V2x 5-8	50	100	7 No.10 + 2 No.8	7 No.10 + 2 No.8	4 No. 3 @ 10	4 No. 3 @ 20
	V3x 9-12	45	90	7 No.10	6 No.10	4 No. 3 @ 15	4 No. 3 @ 20
	V4x 13-15	35	75	4 No.10	4 No.8	2 No. 3 @ 15	2 No. 3 @ 25
	V1y 1-4	60	115	8 No.12 + 2 No.10	8 No.12	6 No. 4 @ 20	6 No. 4 @ 25
	V2y 5-8	55	110	7 No.12 + 2 No.10	7 No.12	4 No. 4 @ 15	4 No. 4 @ 20
	V3y 9-12	55	100	7 No.12	6 No.12	4 No. 4 @ 20	4 No. 4 @ 25
	V4y 13-15	45	85	6 No.10	5 No.10	4 No. 3 @ 20	4 No. 3 @ 30
Columns	**Story**	**B**	**h**	**Flexural rebars**	**Rebar ratio**	**End stirrups**	**Center stirrups**
	C1 Ext 1-5	135	135	52 No. 12	3.25%	8 No. 4 @ 10	8 No. 4 @ 20
	C2 Ext 6-10	120	120	40 No. 10	2.20%	6 No. 4 @ 10	6 No. 4 @ 20
	C3 Ext 11-15	105	105	24 No. 10	1.72%	5 No. 4 @ 10	5 No. 4 @ 20
	C1 Int 1-5	115	115	48 No. 10	3.14%	8 No. 3 @ 10	8 No. 3 @ 20
	C2 Int 6-10	110	110	40 No. 10	3.17%	6 No. 4 @ 10	6 No. 4 @ 20
	C3 Int 11-15	100	100	28 No. 10	3.07%	6 No. 3 @ 10	6 No. 3 @ 20

To minimize the potential formation of soft or weak stories, there were not simultaneously changes of cross sections in any story for beams, columns, and bracing elements. The beams present different mechanical and/or geometrical properties according to the analysis direction, since the length between bays are different for both directions (Fig. 2). The columns differ according if they were connected to the bracing-HEDD system (exterior columns), with those that were not (interior columns). The 15-story model has greater cross sections for beams in *y*-direction and they have even up to 40% greater area with respect to the beams in *x*-direction for the same story. As the model increases in height, these differences decrease, since the strength requirements usually are smaller (Table 3). Exterior columns from the 15-story building used the special load combination just described above, since the building's global slenderness ratio is H/L > 2.5. The area of the

cross section, resulting from the design process, was greater in a 40%, in comparison with the interior columns for the same story. In any case, the rebar ratio for the columns does not exceed the 4%.

The design process takes into account SSI, structural elements under the ground level were designed and modeled in order to create the caisson foundation. Compressive strength for those RC elements was identical to the elements above the ground. Likewise, the beams have different cross sections in both directions, but they are the same as the first story in Table 3 (*V1x* and *V1y*); nevertheless, the beams under the ground used a minimum amount of rebars. The columns used the same criteria in the basement, same cross sections from the first story but with a reduced amount of rebar ratio. In addition, the perimeter RC walls used a greater thickness in the *y*-direction. Finally, below each column there are groups of nine piles. The foundation of the eight-story building used friction piles of 10 m length, with the same geometric and mechanical properties regardless of whether or not they were under the exterior or interior columns. For the 15-story and 24-story buildings, the length of the piles extent until the rock layer (Table 4).

Table 4 – Structural elements for the 15-story building's basement (units: cm)

	Basement	**b**	**h**	**Top rebar**	**Bottom rebar**	**End stirrups**	**Center stirrups**
Beams	VSx	50	100	6 No.8	5 No.6	3 No. 3 @ 15	3 No. 3 @ 25
	VSy	60	115	8 No.8	6 No.8	6 No. 3 @ 15	6 No. 3 @ 25
Columns		**b**	**h**	**Flexural rebar**	**Rebar ratio**	**End stirrups**	**Center stirrups**
	CS Ext	135	135	44 No. 12	2.75%	8 No. 4 @ 10	7 No. 4 @ 20
	CS Int	115	115	44 No. 8	1.69%	8 No. 3 @ 10	8 No. 3 @ 20
Walls		**t**		**Flexural rebar**	**Shear rebar**		
	BWx	30		2 No.5 @ 40	2 No.4 @ 35		
	BWy	40		2 No.5 @ 30	2 No.4 @ 25		
Piles		**d**		**Piles under a column**	**Length of the pile (m)**	**Length until the rock layer (m)**	
	Exterior	40		9	37.4	51	
	Interior	35		9	37.4	51	

4. Nonlinear static analysis

The results obtained from pushover analyses performed with the software MIDAS Gen, were used to assess suitable global and local seismic design parameter for the resilient design of RC buildings with HEDDs under study. Self-weight, dead loads and a percentage of the live load were taking into account as the initial load condition. Two different lateral load patterns were used: based upon a static load distribution and the fundamental mode of vibration. In addition, P- Δ effects were taken into account for all the pushover analyses. Moreover, soil-structure interaction was included in order to evaluate the nonlinear behavior for the elements below the ground level (walls, beams and columns).

The nonlinear moment-curvature relationships and response envelopes of RC elements were obtained using the confined Kent and Park model [14]. The steel bracing only admits axial load (elastic-perfectly plastic yielding in tension and buckling in compression). The model for HEDDs (ADAS and BRBs) used general link elements with six degrees of freedom, post-yielding stiffness of 5% of the elastic one, and the yielding strength of those elements. All pushover analyses were stopped when the HEDDs developed their peak local ductility demand for design, which it is an indicative value when the devices may disconnect from the bracing system depending on low and large cycle fatigue demands.

The global capacity curves are obtained exclusively in terms of the own structural displacements. The different parameters schematically depicted in Fig. 6 are helpful to understand the capacity curves excluding SSI and that for the foundation. In first instance, the curve labeled "Excluding SSI" denotes the nonlinear participation for the structure only. For this purpose, the displacement generated at ground level (D_o) is removed and the reference base shear that it is used for this curve is at the same level of the before mentioned displacement (V_b). Finally, in the graph named "Foundation", the displacement D_o and the base foundation shear minus the participation at ground level ($V_{basement}$ -V_b) is taking into account.

The global ductility reduction factor (Q) developed by the buildings were lower than those developed by the frames evaluated in previous work [5]. This behavior is due to the limitation for drift values according to their ultimate and service conditions. With the exception for the 8-story model in the x-direction, all models developed a global ductility between $2.0<Q<4.0$ (Fig. 7). Finally, overstrength factors were greater than the assumed in the design process ($\Omega_0 \approx 1.5$). Global overstrength values are in a range between $1.9<\Omega_0<2.4$. In addition, the value of Ω_0 decrease for buildings with slenderness ratios of $H/L<3.0$ when SSI is taken into account (Figure 7).

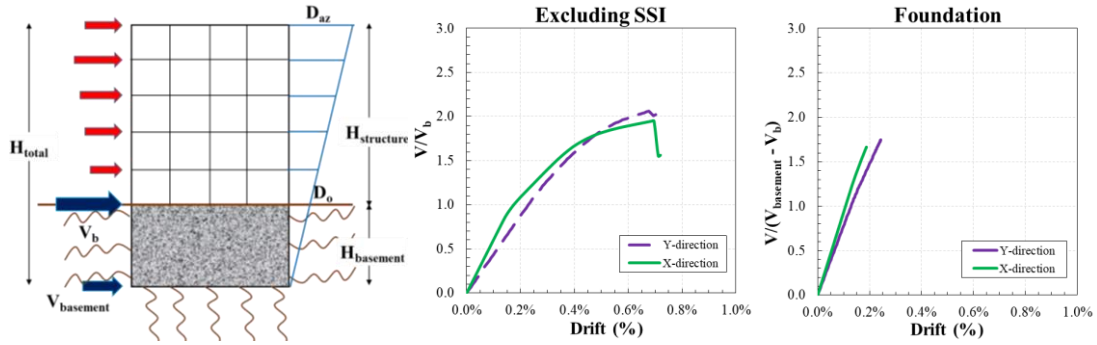

Fig. 6 – Compute of the capacity curves with soil-structure interaction for 15-story model

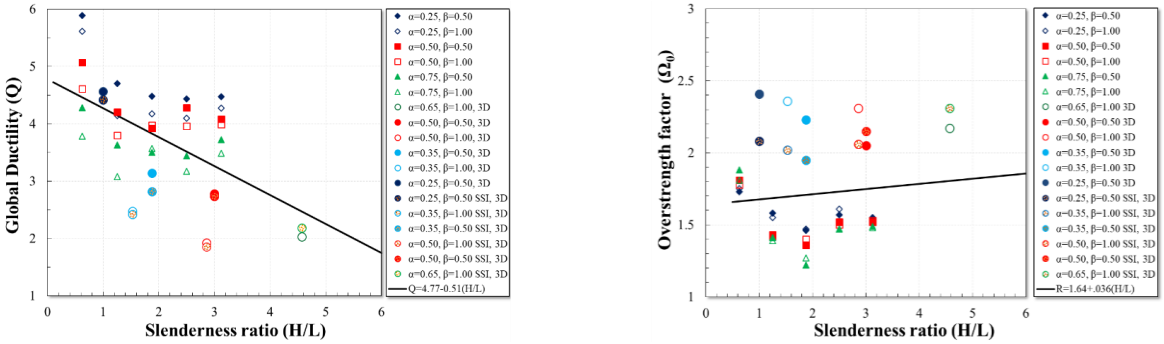

Fig. 7 – Seismic response modification factors for frames and buildings with pushover analysis

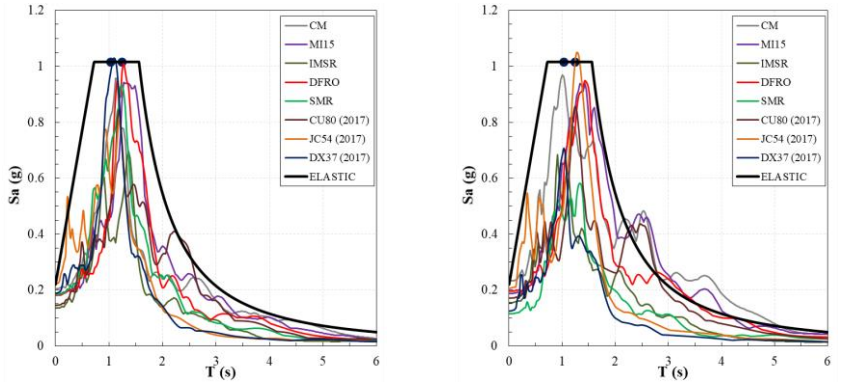

a) EW-direction b) NS-direction

Fig. 8 – Response spectra for the 15-story model

5. Nonlinear time-history analysis

The results obtained with eight pairs of acceleration records for each building, also evaluated the seismic structural behavior for RC buildings with HEDDs. Those records are representative of the soft soil site where the buildings are located and simultaneously applied in order to assess the maximum inelastic response.

Some of them correspond to recorded ground motions of strong earthquakes felt in Mexico City (September 19, 1985 and 2017 earthquakes), and others were artificially generated [16]. Their corresponding pseudo acceleration spectra for 5%, according with the design spectrum, are in Fig. 8. In order to match their peak pseudo-acceleration to the peak of the elastic spectrum, four records were lightly scaled (not shown for space constraints). Scale factors ranged from 1.05 to 1.09, except record IMSR, where a scale factor of 1.46 was used.

In general, hysteretic cycles at the underground levels were linearly elastic manner for both directions and, therefore, the global behavior for the foundation will be elastic as well (Fig. 9). It is worth noting that although soil-structure interaction was modeled using equivalent linear springs, columns, beams and walls at the underground levels were modeled with their nonlinear properties. The stories above the ground level at the *x*-direction developed greater displacements than for the *y*-direction, in other words, more ample inelastic cycles are presented in *x*-direction thus the drift values were greater in this direction too (Fig. 9). Moreover, values of the ratio V/W_T were greater at the *y*-direction; however, as the building increased in height, this value is almost the same for both directions. In general, for the orthogonal direction where peak nonlinear demands were developed, minimum non-linear behavior was expected according to the peak elastic pseudo-acceleration obtained (Table 5), highlighting the fact that extrapolating, *a-priori*, peak nonlinear responses for buildings designed for a large global ductility demands base upon initial elastic properties and peak record demands is not wise enough.

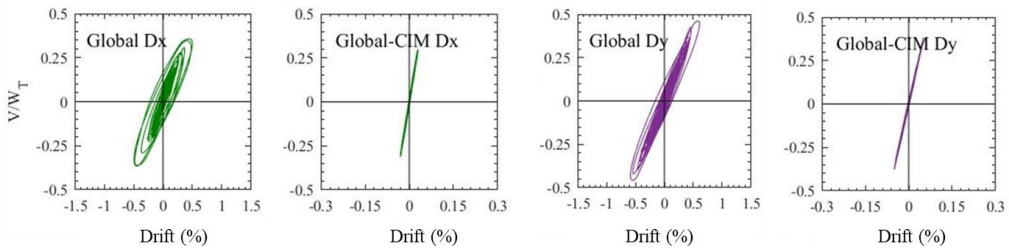

Fig. 9 – Global hysteresis curves for the structure and the basement for the 15-story model

In the graphs shown in Fig. 10, story drifts depicted different limit states for all the buildings with SSI effects modeled. For each particular figure, there are the average responses, the peak response and the design drift (Fig. 10a, 10b). A proposed design story drift value for the service limit state (Δ_y=0.003) was used for the RC buildings with HEDDs, regardless its lateral stiffness ratio α and β. In this case, this drift was associated with the first yielding of any HEDD. However, at the *y*-direction, as studied buildings increased in height, peak drifts increased as well, in some instances beyond the proposed allowable yielding drift (Fig. 10a). Following the same criteria, envelopes for peak story drifts (Δ_{max}=0.015) were computed and are depicted in Fig. 10b. It seems that the proposed drift limit, for a resilient design under the earthquake design scenario, is a good option to avoid even light damage in beams and columns, because in all cases the design drift limit covers peak drifts obtained from the inelastic dynamic analysis.

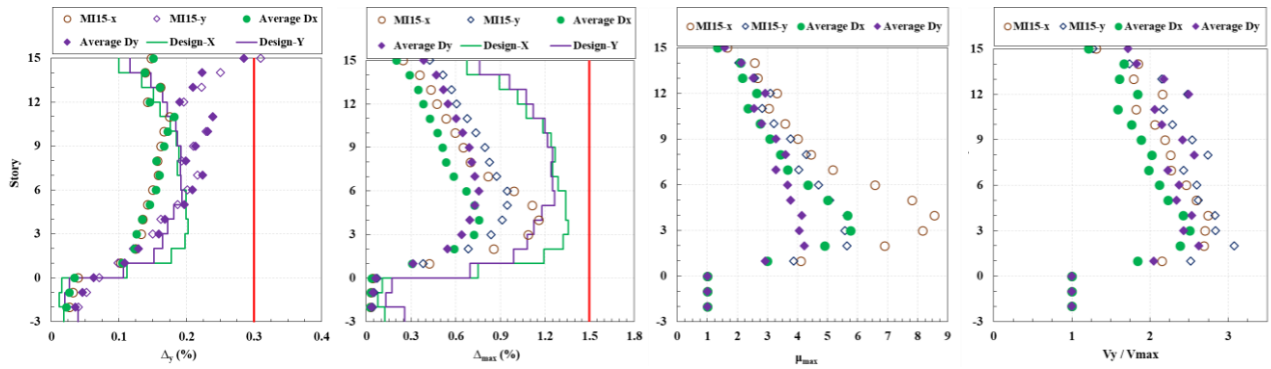

a) Yielding story drift b) Peak story drift c) Story ductility d) Story overstrength

Fig. 10 – Envelopes of peak and average response for 15-story model with SSI

Envelopes of average responses and response maxima, based on the hysteretic story curves and their corresponding results assessed for the 15-story model are shown in Fig. 10c and 10d. It is noticeable that under the action of the pair MI15 acceleration records, the *x*-direction developed the greatest ductility values (μ_{max}), and they were greater up to 54% (Fig. 10c). In other words, the direction with ADAS devices obtained greater ductility demands than in the direction with BRBs. Finally, average developed story overstrengths were very similar among stories two to five between each analysis direction, although these values were between 1.5 <V_y/V_{max}<2.5. The underground stories obtained values of 1.0 for the peak ductility response and for the overstrength factors because of their elastic behavior (Fig. 10d).

6. Inelastic demand mappings

Inelastic demand mappings depict the damage that each considered structural elements would develop according to their accumulated inelastic rotation. With these figures, it is possible to visualize how and where peak rotations for HEDDs, beams and columns developed. In order to represent these inelastic rotations, nine different colors depict the percentage of non-linear behavior for the RC elements. Those colors denote a percentage of the maximum rotation that each element could developed computed with the following formula:

$$\theta(\%) = \frac{\theta - \theta_y}{\theta_u - \theta_y} \tag{2}$$

Therefore, the white code represents an incipient inelastic behavior; the black code represents a rotation close to their maximum bending rotation or a plastic hinge; the other codes represent intermediate points between the yield point and the last point. Finally, when for an elastic behavior in the structural element there is any graphic representation, which it is the case for all the steel bracing elements in all the models evaluated.

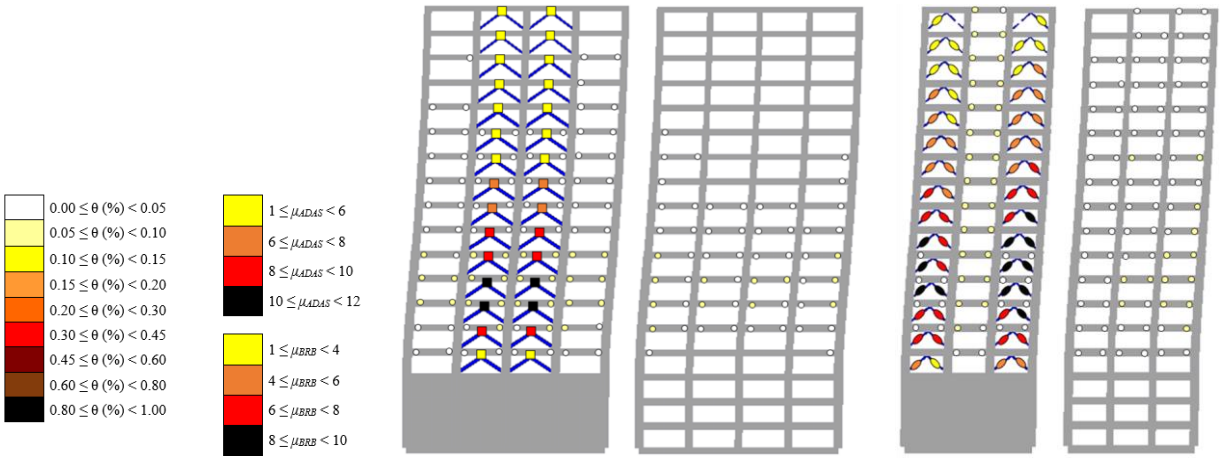

a) Color code b) *x*-direction c) *y*-direction

Fig. 11 – Inelastic demand mapping for the interior and exterior frames of the 15-story model when subjected to the pair of MI15 acceleration records

The inelastic demand mappings shown in Fig. 11 are representative of the results obtained with the pair of acceleration records for station MI15 during the September 19, 2017 earthquake, although peak rotations do not occur at the same time-step. For all the evaluated models, most of the nonlinear behavior is concentrated in the HEDDs (structural fuses) and peak ductility occurred at stories three to six (Fig. 11). However, there were some incipient nonlinear yielding in some beams at the exterior and interior frames, although the inelastic participation of these beams were less than 10% of the ultimate rotation capacity for the RC section where the ADAS or BRBs developed their peak ductility demand (Fig. 11). Moreover, pushover and nonlinear time-history demand mappings are similar between them; even though, the local ductility

developed for HEDDs are less with nonlinear time-history analysis, especially for the last half of the building.

In past earthquakes, some structures have had to be demolished due to the great magnitude of their permanent lateral deformations, even when the structures did not show partial collapse or severe damage in their structural components. Then, residual drifts are also an important parameter to evaluate. For this research, in order to model the free vibration response, the acceleration record added fifteen seconds of zeros at the end. In addition, a ratio between the residual drift at the end of the motion (d_r) and maximum possible residual drift ($d_{r,max}$) was measured. The last one is the residual drift, which occurs immediately after the discharge happens when the cycle develops its peak lateral displacement (Fig. 12a). As Henry and collaborators comment, McRae and Kawashima originally proposed this behavior known as “shake-down” phenomenon, in 1997 [17]. For 15-story model with SSI, the average response d_r is greater than the peak response with acceleration records MI15 at the *x*-direction (Fig. 12b). On the contrary, the average residual drifts at the *y*-direction are greater up to the fifth story, with a peak residual drift of 0.0063%. In addition, average values for the ratio d_r / $d_{r,\,max}$ were up to 55% up to the third story when considering SSI effects. However, this ratio is still less than 5% of the peak residual drift immediately after unloading, and for the most unfavorable case, this parameter increased up to 10% for the last story at the y-direction (Fig. 12b). It is important to mention that although there were amplifications taking into account the SSI in the buildings, these values still do not depict a problem for the operability after a major earthquake, even when the HEDDs develop their peak ductility.

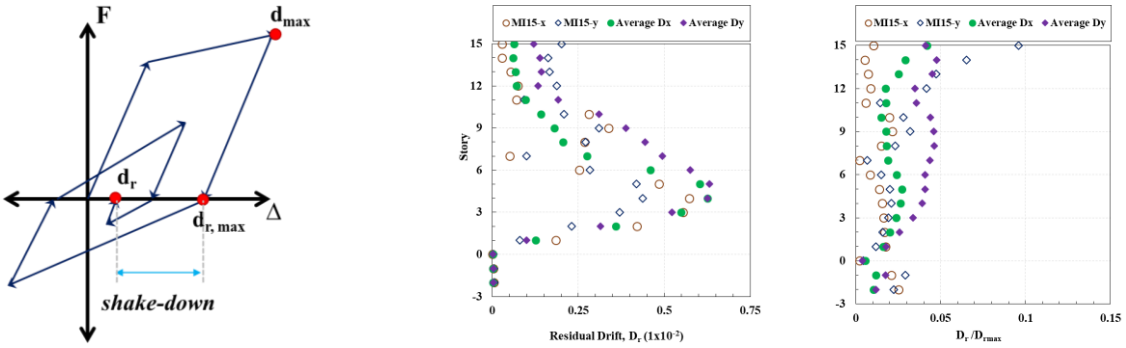

a) Dynamic shake-down behavior (Adapted) b) Absolute and normalized residual drifts

Fig. 12 –Residual drifts for 15-story model with SSI under the action of the pair of MI15 records

7. Concluding Remarks

Based on the results obtained from 3D nonlinear dynamic analyses, a resilient structural behavior was observed for almost all the models evaluated (with slenderness ratio H/L<4.0) using the proposed 100% code-oriented design methodology briefly described in this paper. The nonlinear behavior was focused on ADAS and BRBs devices; in fact, the HEDDs exhibited excellent hysteretic behavior. From the inelastic demands mappings, in all cases the columns and bracings remained elastic. However, some beams exhibited incipient yielding, especially in the frames where HEDDs were located. In most cases, the maximum rotation were lower than 15% of the ultimate one (H/L > 4.0), and they are associated with secant stiffness of 85% of the elastic ones. Nevertheless, the residual rotations decreases significantly and, in some cases, they are negligible, so the expected and observable damage would correspond to cracks of minimal thicknesses and easily repairable.

The drifts related to damage control did not exceed the proposed allowable drift (Δ_u=0.015), even for the peak responses. From the results obtained with the nonlinear time-history analyses, the ductility demand of the buildings (μ=Q), ranged between 3.1<Q<5.6. The values for overstrength ranged between 1.9 <Ω_0<3.4, and they were higher than those assumed in the design process. Although in some cases peak ductility demands and drifts exceeded the assumptions from the design, the residual drifts reported after the

earthquake ends were insignificant (d_r = 0.024%). In other words, after the seismic event, buildings with HEDDs have a low probability to remain with a visible permanent lateral deformation that require the operation close in order to evaluate the structural safety. Finally, it can be concluded that the design methodology (based on stiffness ratios between frame system and bracing-HEDD system), and the use of global design seismic parameters proposed was successful to achieve resilient seismic performances.

8. Acknowledgements

The PhD fellowship granted to the author by the National Science and Technology Council of Mexico (CONACYT) is gratefully acknowledged.

9. References

[1] Martinez-Romero, E (1993): Experiences on the use of supplementary energy dissipators on buildings structures. *Earthquake Spectra*, **9** (3), 581-625.

[2] Tena A (2003): Disipación pasiva de energía en México: un estado del arte. *VII Congreso Nacional de Ingeniería Sísmica*, Barquisimeto, Venezuela.

[3] NTCS-17 (2017): *Normas Técnicas Complementarias para Diseño por Sismo*. Gaceta Oficial de la Ciudad de México, No. 220-BIS, diciembre

[4] Tena-Colunga A, Nangullasmú-Hernández HJ (2015): Assessment of seismic design parameters of moment resisting RC braced frames with metallic fuses. *Engineering Structures*, **95** (15), 138-153.

[5] Nangullasmú-Hernández HJ, Tena-Colunga A (2017): Importance of ductile confinement in reinforced concrete frames with structural fuses. *16th World Conference on Earthquake, 16WCEE*, Santiago, Chile.

[6] Riobóo JM (1995): Estructuras de Concreto. *Simposio Internacional: La ingeniería civil a 10 años de los sismos de 1985*, Ciudad de México, México.

[7] Tena-Colunga A, Correa-Arizmendi H, Luna-Arroyo JL, Gatica-Avilés G (2008): Seismic behavior of code-designed medium rise special moment-resisting frame RC buildings in soft soils of Mexico City. *Engineering Structures*, **30**, 3681-3707.

[8] Nangullasmu H (2019): Comportamiento sísmico de edificios de concreto reforzado con disipadores histeréticos. Propuesta de diseño resiliente conforme a reglamento. *Tesis de Doctorado*, División de Ciencias Básicas e Ingeniería, Universidad Autónoma Metropolitana Azcapotzalco, México.

[9] NTCC-04 (2004): *Normas Técnicas Complementarias para Diseño de Estructuras de Concreto*. Gaceta Oficial de la Ciudad de México, Tomo II, No. 103-BIS, octubre.

[10] Tena-Colunga A (1997): Mathematical modelling of the ADAS energy dissipation device. *Engineering Structures*, **19**, 811-821.

[11] Vargas RE, Bruneau M (2006): Analytical investigation of the structural fuse concept. *Rep. No. MCEER-06-004*, Multidisciplinary Center for Earthquake Engineering Research, State Univ. of New York at Buffalo, Buffalo, N.Y.

[12] NTCS-04 (2004): *Normas Técnicas Complementarias para Diseño por Sismo*. Gaceta Oficial de la Ciudad de México, Tomo II, No. 103-BIS, octubre.

[13] Godínez-Domínguez EA, Tena-Colunga A, Pérez-Rocha LE (2012): Case studies on the seismic behavior of reinforced concrete chevron braced framed buildings, *Engineering Structures*, **45**, 78-103.

[14] Park R, Paulay T (1975): *Reinforced Concrete Structures*, John Wiley & Sons, 1st edition.

[15] Godínez, E A (2005), "Evaluación de la vulnerabilidad sísmica de estructuras existentes en el Distrito Federal. El caso específico del sismo del 19 de septiembre de 1985", *Tesis de Maestría*, Posgrado en Ingeniería Estructural, División de Ciencias Básicas e Ingeniería, Universidad Autónoma Metropolitana Azcapotzalco, México.

[16] Henry RS, Sritharan S, Ingham JM (2016): Residual drift analyses of realistic self-centering concrete wall systems, *Earthquakes and Structures*, **10**, 2, 409-428.

